JACS
JOURNAL OF THE AMERICAN CHEMICAL SOCIETY

Article

pubs.acs.org/JACS

Asymmetric Noncovalent Synthesis of Self-Assembled One-Dimensional Stacks by a Chiral Supramolecular Auxiliary Approach

Subi J. George,[†,‡] Robin de Bruijn,[†] Željko Tomović,[†] Bernard Van Averbeke,[§] David Beljonne,[§] Roberto Lazzaroni,[§] Albertus, P. H. J. Schenning,[†,*] and E. W. Meijer[†,*]

[†]Institute for Complex Molecular Systems and Laboratory of Macromolecular and Organic Chemistry, Eindhoven University of Technology, P.O. Box 513, 5600 MB Eindhoven, The Netherlands

[‡]New Chemistry Unit, Jawaharlal Nehru Center for Advanced Scientific Research (JNCASR), Jakkur P.O., Bangalore 560064, India

[§]Service de Chimie des Matériaux Nouveaux, Université de Mons (UMONS), Place du Parc 20, 7000 Mons, Belgium

Supporting Information

ABSTRACT: Stereoselective noncovalent synthesis of one-dimensional helical self-assembled stacks of achiral oligo(*p*-phenylenevinylene) ureidotriazine (AOPV3) monomers is obtained by a chiral supramolecular auxiliary approach. The racemic mixture of helical stacks of achiral AOPV3 molecules is converted into homochiral helical stacks, as shown by both spectroscopic measurements and molecular modeling simulations. The conversion is promoted by an orthogonal two-point ion-pair interaction with the chiral auxiliary dibenzoyl tartaric acid (D- or L-TA) molecules, which biases the angle population distribution and thereby the stack helicity. The induced preferred helicity is maintained by the OPV stacks even after the removal of the chiral auxiliary by extraction with ethylenediamine (EDA), due to the kinetic stability of the OPV stacks at room temperature. Spectroscopic probing of the helical self-assembly and the racemization process of these π-conjugated OPV chromophores shed further light into the mechanistic pathways of this chiral asymmetric noncovalent synthesis and the kinetic stability of the stacks produced. The racemization of the stacks follows first-order kinetics and no switch in mechanism is observed as a result of a temperature change; therefore, a racemization via disassembly assembly is proposed. Remarkably, the preferred helicity of the stacks of achiral AOPV3 can be retained almost completely after a heating−cooling cycle where the stacks first partially depolymerize and then polymerize again with the still existing stacks being the seeds for self-assembly of achiral AOPV3. Only after a fully dissociated state is obtained at high temperatures, the optical activity of the supramolecular stack self-assembled at room temperature is lost.

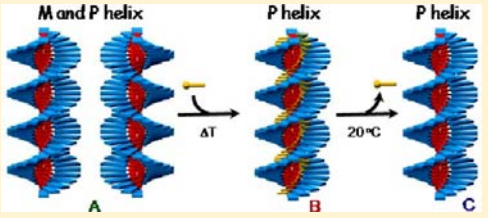

INTRODUCTION

Chirality is an intriguing topic in different scientific disciplines ranging from the enantiomerically pure drug and the origin of biomolecular chirality via helical synthetic polymers and supramolecular systems to the separation of racemic compounds.[1−3] Where asymmetric synthesis of organic compounds has become a very successful field of chemistry by itself, the asymmetric noncovalent synthesis is only at its beginning. The full control of chirality at the different hierarchical states of self-assembled structures and the transfer, amplification, and storage of this chirality is of great interest.[4] Within this area, the formation of an assembly constructed from achiral building blocks, but containing a preferred handedness of its supramolecular chiral state is a real challenge and is defined as the asymmetric noncovalent synthesis of self-assembled structures.[5] Successful approaches require a kinetic stability of the self-assembled state that is high enough to isolate the homochiral structure formed. In this respect, helical one-dimensional stacks are an appealing class of bottom-up systems that resemble many aspects of biomolecules, synthetic polymers, and crystals.[6]

In earlier studies, chiral supramolecular auxiliaries have been used to bias the chirality of racemic covalent polymers.[7] In most cases, the chiral auxiliary had to be replaced by achiral analogues to stabilize the helical polymer.[8,9] In an achiral polyisocyanide, a preferred helicity was induced by an optical active amine and this helicity was maintained after removal of the auxiliary.[10] The use of supramolecular auxiliaries to noncovalent systems is rare because of the fast dynamics of these self-assembled objects. Furthermore, auxiliaries can interfere with the interactions that hold the self-assembly together and are not easy to remove from the reaction mixture, without affecting the self-assembly process due to kinetic instability of the product. Supramolecular chirality has been induced in achiral self-assemblies by chiral guest molecules[11−15] or solvents.[16] However, in only a few examples, the often called "memory approach" has been reported in which the conformational inertness of the kinetically trapped chiral architecture is sufficient to overcome the removal or substitution of the auxiliary.[17−21] Asymmetric synthesis of

Received: August 30, 2012
Published: October 2, 2012

dx.doi.org/10.1021/ja3086005 | J. Am. Chem. Soc. 2012, 134, 17789−17796

discrete supramolecular calixarene-based double-rosettes has been reported in which chiral monomers were substituted by achiral ones.[17a] Self-assembled chiral memory systems have also been constructed from achiral porphyrins.[18] Interestingly, after removal of the chiral template, the porphyrin aggregates remember their helicity, which could be released and restored by changing the pH.[19,20] Recently, we have described porphyrin-based supramolecular copolymers that show chiral amplification, selective disassembly (or depolymerization) and chiral memory. The chiral information in the porphyrin aggregate is retained due to low conformational dynamics, which also allows temperature-induced switching of the chiral memory.[21] We now report the full control of chirality in one-dimensional self-assembled stacks (Scheme 1) by using a supramolecular chiral auxiliary approach: a racemic mixture of helical stacks of achiral molecules is converted into homochiral assemblies. After removal of the auxiliary, the helicity in these stacks remains intact and even after partial disassembly, the helicity is recovered upon reassembly. Racemization studies reveal the temperature and concentration range for the use of the chiral auxiliary strategy in which the helical stacks are kinetically stable. In general, our approach represents a new tool to create helical one-dimensional self-assembled systems.

Scheme 1. Molecular Structures of the Achiral OPV (AOPV3) and the Enantiomeric Dibenzoyl Tartaric Acid (D-TA and L-TA) Derivative Chiral Auxiliaries[a]

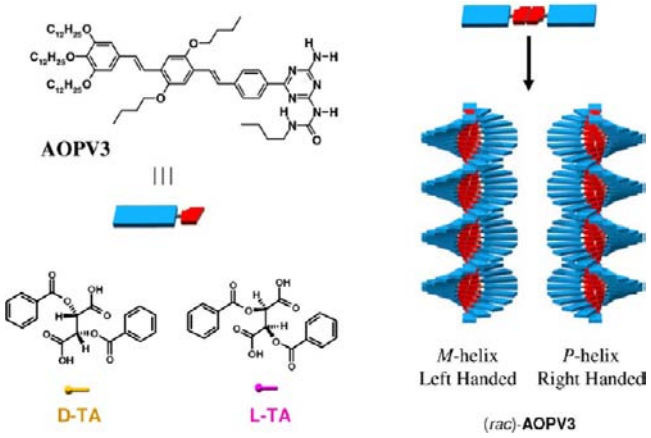

[a]Schematic representation of the self-assembly of AOPV3 to racemic helical stacks is also shown.

We have been extensively studying the cooperative self-assembly of π-conjugated oligo(*p*-phenylenevinylene)s end-capped with ureidotriazine quadruple-H-bonding motif (OPVs) in apolar solvents.[22] In this hierarchical self-assembly, the OPVs first form H-bonded dimers and subsequent π-stacking to one-dimensional fibrous structures follows a cooperative nucleation–elongation mechanism (Scheme 1); in other words, it is fully homogeneously nucleated.[23] For the temperature-dependent self-assembly, two temperature regimes could be distinguished: the nucleation and the elongation regime, which were separated by the elongation temperature. Above the elongation temperature, mainly H-bonded dimers are present while below self-assembled fibers of H-bonded dimers are formed (Scheme 1). In the case of chiral monomers, one-dimensional stacks with a preferred helicity were formed while chiral induction in racemic self-assemblies of an achiral OPV derivative was achieved by an orthogonal H-bonded recognition of enantiomeric citronellic acid molecules.[11] These stacks are thermodynamically stable at room temperature, making these stacks attractive for the use of supramolecular auxiliaries that can be removed after the self-assembly process. In the present study, we have applied dibenzoyl tartaric acid (TA), because this chiral supramolecular auxiliary has enough solubility in methylcyclohexane (MCH; the solvent of choice for OPV self-assembly) and can be easily removed by amine extraction without affecting the OPV stacks (Scheme 1). This two-step method was recently successfully used in a detailed kinetic study, where even the opposite P-handedness was imprinted into the chiral S-OPV structures.[24] Here we extend this new two-step process to create chiral supramolecular structures from achiral molecules and show that even after partial disassembly; the helicity is recovered upon reassembly. The results are strengthened by molecular modeling simulations.

RESULTS AND DISCUSSION

Step One of the Two-Step Synthetic Approach. The first step toward asymmetric noncovalent synthesis is the induction of a preferred helicity in the otherwise racemic mixture of stacks of achiral OPV molecules AOPV3 by the complexation of D- or L-tartaric acid (D- or L-TA) in MCH during the self-assembly process (Scheme 1). In order to self-assemble the components under thermodynamic control, mixtures of AOPV3 (1×10^{-4} M) and TA (0–2 equiv.) in MCH were heated to the molecularly dissolved state and then cooled down slowly at a rate of 60 K/h. TA binds strongly to OPV and the strong acid–base interaction of the chiral auxiliaries becomes apparent from the optical properties of OPV self-assemblies. In presence of TA molecules, a new weak absorption appears at λ = 525 nm with a red-shift of the absorption maximum (410 to 418 nm), corresponding to the acid–base host–guest complex (Figure 1a). This shift in absorption is in addition to the characteristic features of self-assembled chromophores such as a strong vibronic shoulder at 460 nm. Furthermore, quenching of the self-assembled OPV emission (λ_{em} = 523 and 547 nm) occurs with the appearance of the new emission at λ_{em} = 630 nm (Figure 1b). These changes in optical properties are even visible with the naked eye (insets of Figure 1a,b). Remarkably, the quenching of OPV emission occurs even with low equivalents of the guest molecules (0–0.2 equiv.), which suggests that the low lying excited state of the OPV-TA complex acts as an energy trap in the stacks and energy transfer from the self-assembled OPV molecules can reach this trap (Figure S1 of the Supporting Information, SI). Energy transfer within the stacks is further confirmed by fluorescence lifetime measurements and is similar to earlier reported energy transfer in mixed supramolecular stacks of OPVs with different backbone lengths (Figure S2 of the SI).[25] Interestingly, similar changes in the optical properties were also observed when trifluoroacetic acid (TFA) is added to the OPVs, suggesting that the TA-induced changes are similar to the protonation of the more basic inner face nitrogen of the triazine ring of AOPV3 (Figure S3 of the SI). This has been further investigated by NMR titration of AOPV3 (1 mM) with D-TA intoluene-d8, a good solvent for OPVs. Since the OPV molecules are present as hydrogen-bonded dimers at this concentration, any further changes in NH resonances will give an indication about the binding of auxiliary molecules. The free NH proton on the triazine ring, which is not involved in the quadruple H-bonding interaction, showed a significant down-field shift in the presence of the acid, which is a definitive proof

dx.doi.org/10.1021/ja3086005 | J. Am. Chem. Soc. 2012, 134, 17789–17796

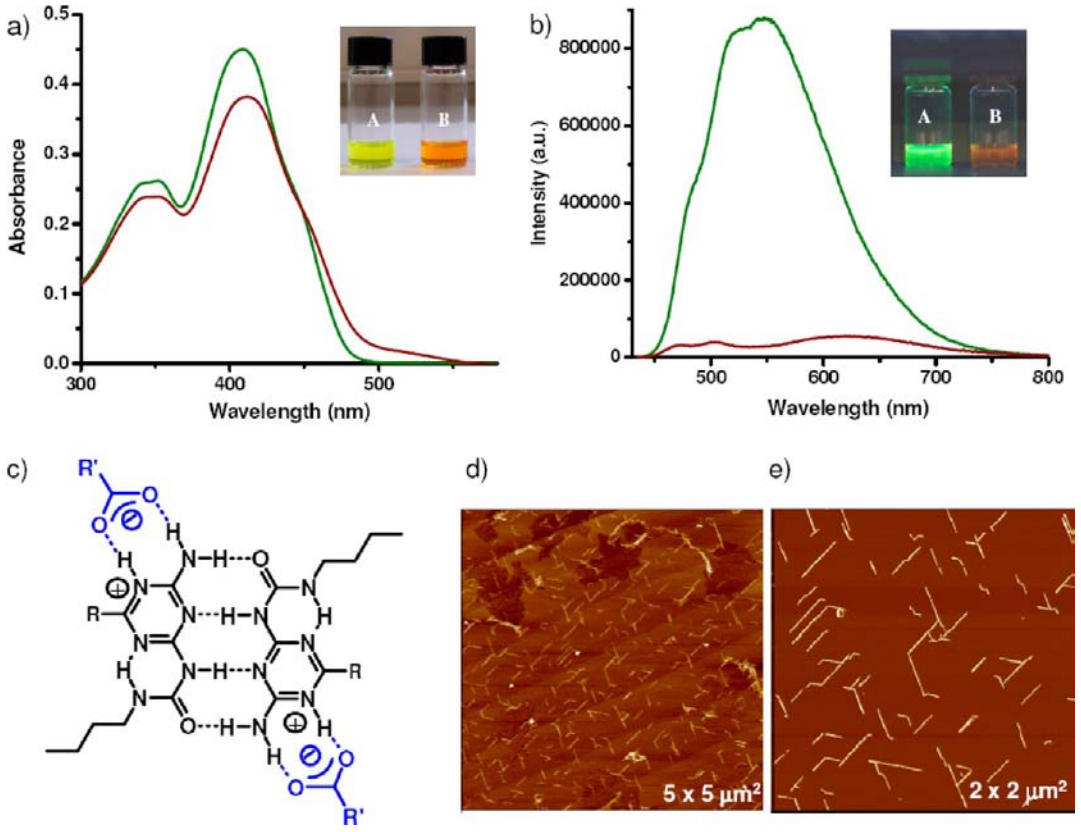

Figure 1. (a) Absorption and (b) fluorescence spectra of AOPV3 (1×10^{-4} M) (green) and AOPV3 + 0.6 equiv. of the D-TA (red) in MCH. Inset of part (a) shows the corresponding visual changes on AOPV3 solution in MCH upon TA binding while the inset in part (b) shows the fluorescence changes upon irradiation with UV light (λ = 254 nm); (A) AOPV3, (B) AOPV3 + D-TA. (c) Proposed hydrogen-bonded ion-pair structure of AOPV-TA complex. Parts (d) and (e) are height and phase AFM images of one-dimensional stacks formed in MCH measured on a mica substrate.

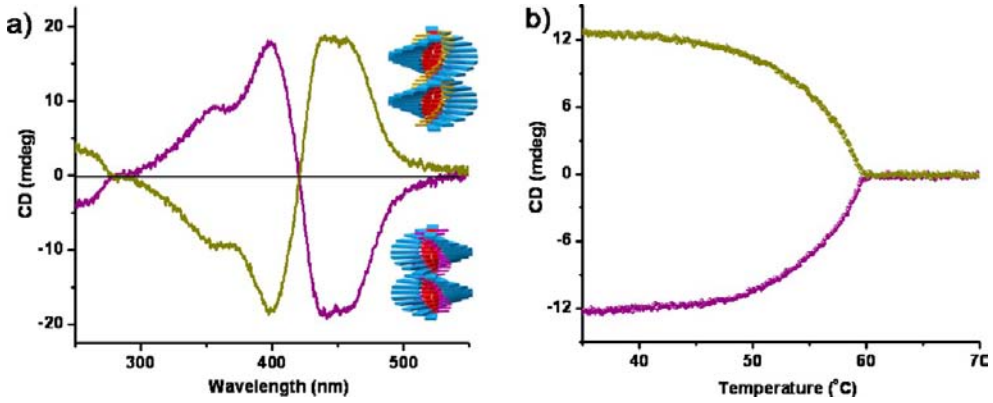

Figure 2. (a) Mirror image CD spectra of AOPV3 (1×10^{-4} M) with 0.6 equiv. of D-TA (yellow spectrum) and L-TA(purple spectrum) in MCH and (b) corresponding cooling curves monitored at λ = 430 nm (dT/dt = −60 K/h, l = 1 mm).

for complexation of D-TA through H-bond type interactions. Furthermore, aromatic protons of the benzene ring near the ureidotriazine motif showed an upfield shift, suggesting a strong interaction of TA molecules through the most basic noncentral triazine ring N atom (Figure 1c) (Figure S4 of the SI). Incidentally, such changes are similar to related triazine systems on protonation, as reported in the literature.[26] NMR experiments further show that the guest binding does not disturb the quadruple H-bonding pattern of the OPV molecules. On the basis of these observations, we propose that the interaction of TA chiral auxiliaries is through a hydrogen bonded ion pair (Figure 1c).[27,28] Atomic force microscopy (AFM) analysis of a drop-casted MCH solution of AOPV3 on mica, showed micrometer long fibers, revealing similar self-assembly as that of reported for helical assemblies of analogous OPVs with chiral side chains (Figure 1d,e).

The interaction of the chiral auxiliary with AOPV3 stacks has been further monitored with circular dichroism spectroscopy (CD). In the absence of the chiral auxiliary, the racemic mixture of *P*- and *M*-helical stacks of achiral OPV in MCH is not optically active as shown by the lack of any CD effect. However, AOPV3 (1×10^{-4} M) in the presence of D-TA or L-TA (0.6 equiv.) showed mirror image bisignate Cotton effects (Figure 2a, Figure S6 of the SI). This indicates that the chiral auxiliaries

dx.doi.org/10.1021/ja3086005 | J. Am. Chem. Soc. 2012, 134, 17789−17796

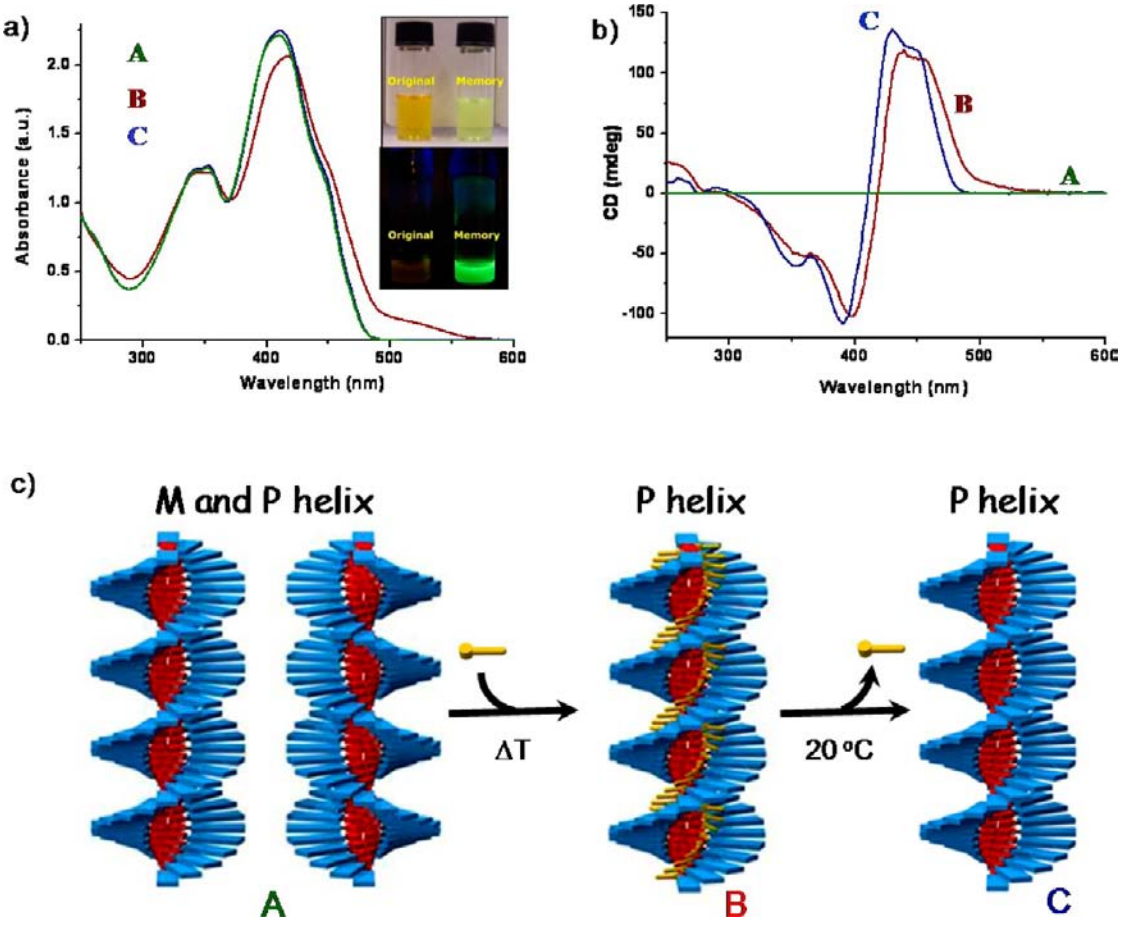

Figure 3. (a) Absorption and (b) CD spectra of the assemblies of racemic (*rac*)-AOPV3 (1×10^{-4} M, l = 5 mm) (A), (*P*)-AOPV3-D-TA (B) and (*P*)-AOPV3 after removal of the chiral auxiliary (C) in MCH. Inset of (a) shows the visual changes in absorption and emission (excited at λ = 254 nm) before and after removal of the chiral auxiliary D-TA. (c) Schematic representation of the asymmetric synthesis of AOPV stacks having a *P*-helicity using a supramolecular chiral auxiliary approach.

induce a preferred handedness in the self-assembled helical stacks of achiral OPV molecules, similar to citronellic acid (CA) derivatives reported earlier.[11] We found that D-TA induces *P*-helicity, as indicated by the positive bisignate signal with a zero-crossing at 418 nm, which is close to the wavelength of the absorption maximum characteristic of exciton-coupled chromophores. Similarly, *M*-helicity is induced by the L-TA. Furthermore, so-called "Majority Rules" experiments[29,30] of AOPV3 by varying the enantiomeric excess (*ee*) of the mixture of D- and L-chiral auxiliaries showed a nonlinear relationship for the CD intensity with *ee*, suggesting chiral amplification in the helical stacks (Figure S5 of the SI). Due to the presence of significant chiral amplification and energy transfer in the self-assembled stacks and the cross-linking of the stacks at higher equivalents of acid (Figure S7 of the SI) the simple determination of the stoichiometry and binding constant of chiral auxiliary complexation was difficult to achieve with spectroscopic titration experiments.

Previously, we have shown that temperature-dependent CD spectroscopy at one particular wavelength is a powerful technique to study the distinct hierarchical stages of the self-assembly process.[23,31] This technique is particularly useful in the present study of asymmetric noncovalent synthesis, since we can monitor the nucleation of OPV-chiral auxiliary complexes and their further elongation to helical assemblies. Analysis of the CD cooling curves obtained by monitoring the CD intensity at 430 nm revealed a cooperative nucleation elongation pathway for the formation of the AOPV3-TA chiral assemblies (Figure 2b). Interestingly, the titration of OPV with TA auxiliaries has shown an increase in the stability of the stacks compared to that of the pure racemic AOPV3 stacks, as evident from the increase of elongation temperature, (T_e = the temperature at which elongation of the self-assembly sets in; Figure S8 of the SI). This suggests the possibility of the diacid functionality of the auxiliary molecule acting as a clip between adjacent OPV molecules in the π-stack direction, providing additional stabilization (vide infra).[32] Saturation of increase of T_e at 0.5 equiv. might be an indication of this clip action is based on a 2:1 stoichiometry. This is further supported by the favorable conformation of TA derivatives in presence of H-bond donors[33]and the titration studies with monofunctional tartaric acid derivative, which did not show any significant changes in the T_e (Figure S9 of the SI).

Step Two of the Two-Step Synthetic Approach. Having understood the chiral induction and mode of complexation of TA chiral auxiliary molecules with the original racemic stacks of AOPV3, we moved to step two in the noncovalent synthesis of enantiomerically pure assemblies of AOPV3 by removal of the chiral auxiliary molecules without disrupting the helical assembly (Figure 3). This removal of the chiral auxiliaries was carried out at room temperature by an aqueous extraction with ethylenediamine (EDA, see Experimental Section).

dx.doi.org/10.1021/ja3086005 | J. Am. Chem. Soc. 2012, 134, 17789−17796

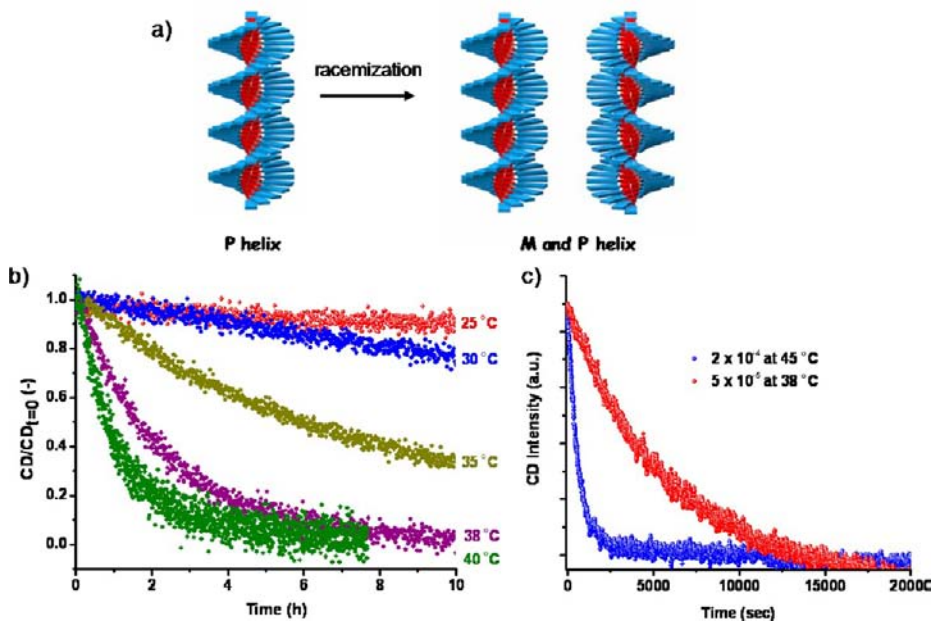

Figure 4. (a) Schematic representation of the racemization process of (*P*)-AOPV3 stacks. (b) Time dependence of CD intensity of the enantiomeric (*P*)-AOPV3 stacks at λ = 430 nm monitored at different temperatures, which shows the racemization process (c = 1 × 10^{-4} M, l = 1 mm). (c) Kinetics of racemization of AOPV3 memory monitored at 45 °C for 2 × 10^{-4} M and at 38 °C for 5 × 10 $^{-5}$ M.

Removal of the acid was again visible with the naked eye (Figure 3a, inset), because the OPV solution regains its greenish emission. The removal of chiral auxiliary could also be monitored by optical spectroscopy and by chiral HPLC (Figure S10 of the SI). In Figure 3, trace A shows the chiroptical properties of (*rac*)-AOPV3 stacks in MCH (1 × 10^{-4} M, λ_{max} = 410 nm) which is CD inactive. The chiral auxiliary induced helical assembly (*P*)-AOPV3-D-TA has a red-shifted absorption (λ_{max} = 418 nm) and right-handed helicity as described before (trace B). After the extraction with EDA, the absorption spectrum of the helical assembly (*P*)-AOPV3 in MCH becomes similar to that of the (*rac*)-AOPV3 (trace C), but (*P*)-AOPV3 retains its right-handed helicity as indicated by the positive bisignate signal with a zero crossing at 410 nm. It should be noted that the CD spectrum of (*P*)-AOPV3-D-TA assembly is red-shifted compared to that of the resulting (*P*)-AOPV3 stacks, suggesting that the helical orientation of molecules in these stacks is different due to the complexation of the chiral auxiliary molecules. The absorption spectrum of the homochiral assembly is, upon the removal of chiral auxiliary, however, similar to a racemic mixture of AOPV3 stacks suggesting that the OPV have a similar orientation.[34] Our data show the successful removal of the auxiliary without disrupting the self-assembly process of the (*P*) helicity of the supramolecular stacks of achiral AOPV3. Although the sign is opposite, the chiral anisotropy factor g of this (*P*)-AOPV3 stack is comparable in size as the g value of the (*M*)-stack of the chiral (*S*)-OPV3 containing chiral *S*-2-methylbutoxy side chains (Figure S11 of the SI); therefore, the enantiomeric excess in this asymmetric noncovalent synthesis is estimated close to 100%, but is obviously dependent on the kinetic stability and history of the sample (vide infra).

Kinetic and Thermodynamic Analyses. In order to determine the temperature and concentration window of the supramolecular auxiliary approach, detailed kinetic and thermodynamic studies have been performed on (*P*)-AOPV3 self-assemblies to get an insight into its kinetic stability. In order to quantify the kinetic stability, the kinetics of racemization of the imprinted (*P*)-AOPV3 stacks (1 × 10^{-4} M) were studied by monitoring the time dependence of CD intensity at λ = 430 nm at different temperatures (Figure 4a,b). The racemization of the stacks follows first-order kinetics and the Arrhenius plot gives a straight line, indicating a single rate-limited thermally activated process (Figure S13 of the SI). There could be two mechanistic pathways for the racemization process; either through an intracolumnar atropisomerization process similar to covalent helical polymers or through an intercolumnar process, which involves the monomers through disassembly and assembly. Most likely, the latter process dominates at elevated temperatures close to the elongation temperature. Since no sudden switch in rates is observed as a function of temperature, it is proposed that the racemization occurs via a dissociation−association mechanism at all temperatures presented here. At room temperature (25 °C), the CD intensity is hardly decreased even after 10 h, indicating that the (*P*)-helical stacks are kinetically stable and its racemization is slow, thereby imprinting a lasting helical memory to the one-dimensional OPV assemblies. At higher temperatures, the kinetic stability decreases and racemization was observed. Monitoring the kinetics of racemization at similar stack lengths, i.e., a similar degree of polymerization where the fraction of monomers and stacks are the same, for two different concentrations (2 × 10^{-4} and 5 × 10^{-5} M, monitored at 45 and 38 °C respectively) showed a faster decay for the higher concentration solution (Figure 4c). This suggests that absolute temperature plays a crucial role in the racemization process, as the assemblies with similar stack length racemize faster at higher temperatures.

Partly Dissociation and Association. Interestingly, due to the kinetic stability of the AOPV stacks, when the heating of an imprinted (*P*)-AOPV3 solution (c = 3 × 10^{-5} M) the dissociation—or depolymerization—is stopped at a certain stack length and cooled back, most of the optical activity and hence the preferred handedness is recovered (Figure 5a).

dx.doi.org/10.1021/ja3086005 | J. Am. Chem. Soc. 2012, 134, 17789−17796

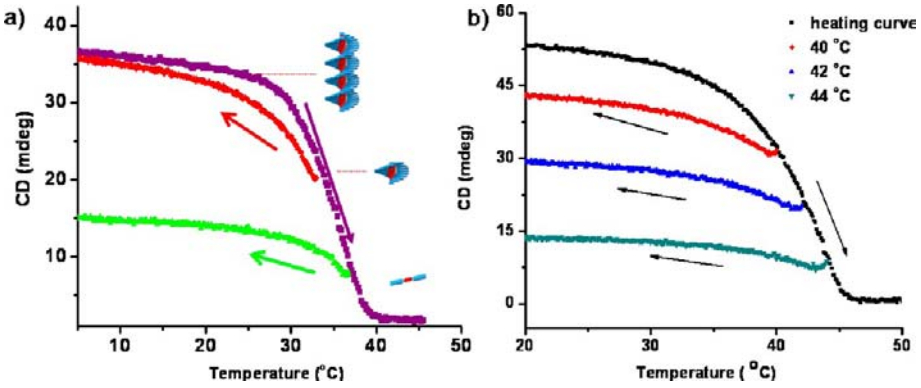

Figure 5. (a) Heating curve of AOPV3 helical memory (purple curve, $c = 3 \times 10^{-5}$ M) and its recovery from 33 °C (red curve) and 37 ° C (green curve). (b) Heating curve of AOPV3 helical memory (black) of 1×10^{-4} M in MCH solution and its recovery from different temperatures.

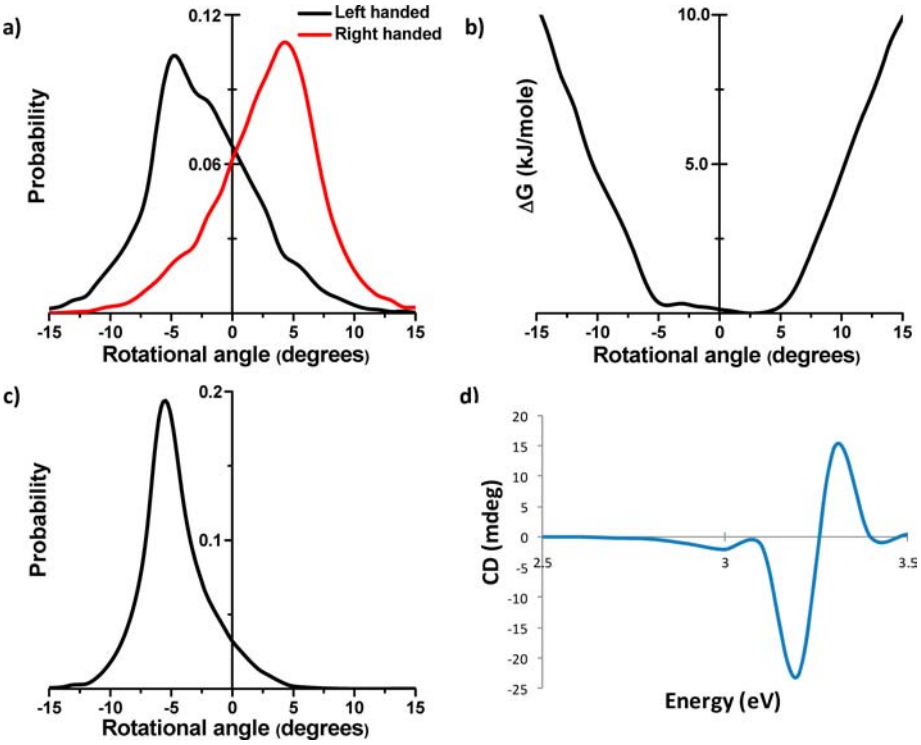

Figure 6. (a) Rotation angle distributions (averaged over the entire MD simulation) for geometries taken from the "no-handed" AOPV3 distribution; (b) corresponding free energy curve; (c) Rotation angle distribution (computed along the entire MD run) for AOPV3+L-TA stack; and (d) Circular Dichroism spectrum computed from MD snapshots.

Hence, the still present shorter stacks act as chiral seeds and amplify the chirality by controlling the handedness of the achiral monomers that grow on top of the stacks.[20,21] The amplification of chiral memory reveals that this process depends on the temperature and concentration. The memory could be completely recovered at longer stack length (cooled from 33 °C, [AOPV3] = 3×10^{-5} M), whereas amplification from short stacks, present close to the T_e (37 °C) was more difficult (Figure S14 of the SI). However, at higher concentration of 1×10^{-4} M, we could not recover the memory completely at any stage of the self-assembly process, probably due to the high temperatures and hence a fast racemization process (Figures 5a and 4b). Other reasons can be found in the need for larger nuclei at lower concentration or due to stochastic phenomena at these lower concentrations. These results show that by choosing the appropriate concentration and temperature range, the reassembly process is able to compete with the racemization and this noncovalent synthesis gives new clues for the amplification of chirality in self-assembly.

Modeling of the Stacks with and without Chiral Auxiliary. The chirality of stacks of 16 AOPV3 dimers was investigated in a molecular mechanics/molecular dynamics (MM/MD) approach using the DREIDING force field method.[35] The MD simulations yield two populations peaking at ∼+5° and ∼−5°, which appear as shoulders in the distributions computed at 150 K and as well-defined dominant peaks in the 298 K distributions (Figures S15 and S16 of the SI). Two such room-temperature distributions are shown in Figure 6, together with the corresponding Gibbs free energy profile obtained by Boltzmann population inversion. We conjecture that the right- or left-twisted structures are stabilized with respect to the cofacial arrangement at 298 K by the larger degree of freedom available to the alkyl side chains and that

dx.doi.org/10.1021/ja3086005 | J. Am. Chem. Soc. 2012, 134, 17789−17796

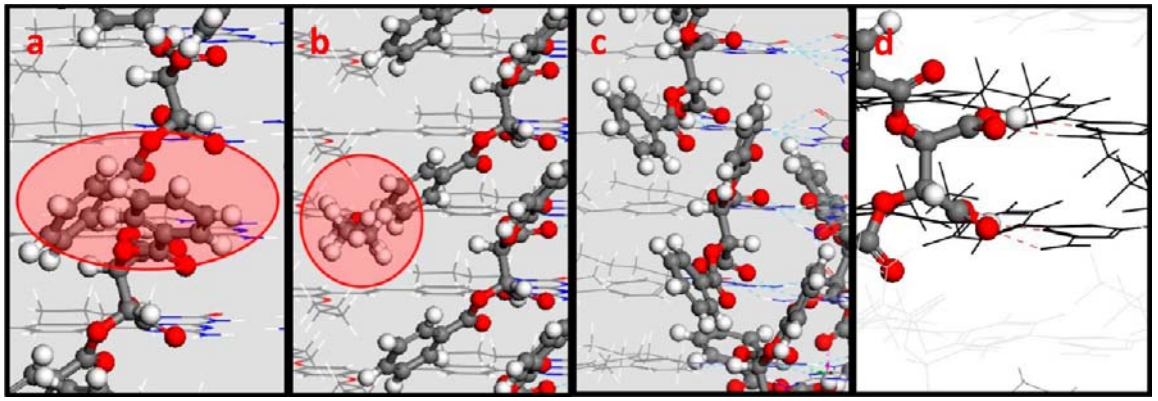

Figure 7. Geometries of right-handed (a) cofacial (b) and left-handed (c) AOPV3 assemblies in the presence of the L-TA molecules; and representation of the "grasp" ability of Tartaric Acids (d). The AOPV3 stack is shown with thin lines while the L-TA molecules are in a "ball-and-stick" representation. Note that in the central structure one side group of one AOPV3 molecule is also represented in "ball-and-stick" to better visualize its interaction with the L-TA molecule.

these can switch back and forth from positive to negative angles due to the relatively low barrier height. These calculations thus suggest that the proper way to envision the stacks of achiral molecules is not based on a cofacial superposition of molecules with zero-degree rotation along the stack but rather as domains with positive and negative rotations that globally average out (as expected from the symmetric shape of the free energy profile in Figure 6).

Next, we have considered the initial geometries of AOPV3 assemblies, to which L-TA molecules have been added, with the constraint that the average rotation angle is maintained. This step is intended to identify the interactions that (de)stabilize the starting geometry and how they impact along an entire MD run. When the most stable structure is unambiguously assigned, the constraint is lifted, the structural evolution of the assembly is followed in terms of rotation angle and a CD spectrum is computed based on snapshots extracted from the MD run. In the presence of the L-TA molecules, the left-handed assembly is the most stable, the cofacial stack being destabilized by 6.1 $kJ{\cdot}mol^{-1}{\cdot}dimer^{-1}$. The destabilization is even much larger for the right-handed assembly: 33.7 $kJ{\cdot}mol^{-1}{\cdot}dimer^{-1}$; a dimer is defined as a pair of AOPV3 molecules plus one L-TA molecule.

These data clearly show that the AOPV3 assembly could be nothing but left-handed in the presence of the chiral auxiliary. The detailed energetic analysis reveals that the destabilization arises from van der Waals interactions between the tartaric acid and the AOPV supramolecular structure. This is better highlighted by Figure 7.

In the case of left-handed helices, the L-TA molecules can efficiently form hydrogen bonds with ureidotriazine fragments of AOPV3 without being perturbed by steric repulsions. As a consequence, all of the interactions are favorable. When one moves to the "co-facial" case, the formation of a hydrogen bond pattern is accompanied by steric repulsion between one aromatic ring of the chiral handle and one side chain of the AOPV3 (highlighted by the red area in Figure7). To overcome this repulsion, the assembly can rearrange by partially breaking the hydrogen bonds or even twisting the AOPV3 structure to move the side chain away. In both situations, the total energy of the system increases. When the entire system is arranged in a right-handed orientation, a steric repulsion appears between the aromatic rings of neighboring tartaric acid molecules (circled in the left panel of Figure 7).The compensation of such repulsion is to entirely break the hydrogen bonds between AOPV3 and the L-TA, or highly twist the L-TA structure. As a consequence, the stabilization effect generated by AOPV3:L-TA interaction is completely lost, making that case the worst one from an energetic point of view. Although we are aware of the prominent role of solvents in the self-assembly processes, these MM/MD calculations strengthen the chiral bias of the auxiliary in the self-assembly of achiral molecules in helical stacks.

■ CONCLUSIONS

The asymmetric noncovalent synthesis of one-dimensional supramolecular polymers by a chiral supramolecular auxiliary approach has been used successfully performed by a two-step process. A chiral auxiliary that interacts in a noncovalent manner with otherwise racemic stacks of achiral molecules gives homochiral stacks even after removal of the chiral auxiliary. The homochiral assembly maintains its handedness due to the kinetic stability of the stacks formed. It even can use its own stacks as seeds to retain its preferred helicity after partly disassembly and reassembly. The chiral auxiliary strategy allowed us to investigate racemization in a one-dimensional supramolecular polymer as function of temperature and concentration. A detailed knowledge of these processes is not only decisive for the use of the supramolecular auxiliaries, but also in understanding homochirality in self-assembled systems. Our work has potentially broad application as an attractive strategy to prepare homochiral assemblies from achiral building blocks in solution as well as at the interface of solvent and a surface.[24]

■ ASSOCIATED CONTENT

Supporting Information

Experimental section and supporting UV−vis, fluorescence, and CD and NMR spectroscopic and modeling figures. This material is available free of charge via the Internet at http://pubs.acs.org.

■ AUTHOR INFORMATION

Corresponding Author

a.p.h.j.schenning@tue.nl; e.w.meijer@tue.nl

Notes

The authors declare no competing financial interest.

■ ACKNOWLEDGMENTS

We would like to thank Prof. Richard Kellogg (Syncom, Groningen, The Netherlands) for stimulating discussions and for providing the tartaric acid derivative. We would like to thank Dr. P.E.L.G. Leclère for the AFM measurements and Ralf Bovee for chiral HPLC measurements. The research leading to these results has received funding from the European Community's Seventh Framework Program under Grant Agreement No. NMP4-SL-2008-214340, project RESOLVE. Research in Mons is also supported by the Belgian Federal Science Policy Office (IAP program), Région Wallonne (Pôled'excellence OPTI2MAT), and FNRS-FRFC. D.B. is FNRS research director. Furthermore, this work is supported by the European Science Foundation (EURYI) and The Netherlands organization for Scientific Research (NWO).

■ REFERENCES

(1) Crego-Calama, M.; Reinhoudt, D. *Top.Curr. Chem.* **2006**, 265.
(2) Green, M. M.; Park, Ji-W.; Sato, T.; Teramoto, A.; Lifson, S.; Selinger, R. L. B.; Selinger, J. V. *Angew. Chem., Int. Ed.* **1999**, *38*, 3138−3154.
(3) Perez-Garicia, L.; Amabilino, D. B. *Chem. Soc. Rev.* **2007**, *36*, 941−967.
(4) Pijper, D.; Feringa, B. L. *Soft. Mat* . **2008**, *4*, 1349−1372.
(5) Purrello, R. *Nat. Mater.* **2003**, *2*, 216−217.
(6) Lee, C. C.; Gernier, C.; Meijer, E. W.; Schenning, A. P. H. J. *Chem. Soc. Rev.* **2009**, *38*, 671−683.
(7) Maeda, K.; Yashima, E. *Top. Curr. Chem.* **2006**, *265*, 47.
(8) Yashima., E.; Maeda, K.; Okamoto, Y. *Nature* **1999**, *339*, 449−451.
(9) (a) Yashima, E.; Maeda, K.; Furusho, Y. *Acc. Chem. Res.* **2008**, *41*, 1166−1180. (b) Yashima, E.; Maeda, K.; Iida, H.; Nagai, K. *Chem. Rev* . **2009**, *109*, 6102−6211.
(10) Ishikawa, M.; Maeda, K.; Mitsutsuji, Y.; Yashima, E. *J. Am. Chem. Soc.* **2004**, *126*, 732−733.
(11) George, S. J.; Tomović, Z.; Smulders, M. M.; de Greef, T. F.; Leclère, P. E.; Meijer, E. W.; Schenning, A. P. H. J. *Angew. Chem., Int. Ed.* **2007**, *46*, 8206−8211.
(12) Fenniri, H.; Deng, Bo-L.; Ribbe, A. E. *J. Am. Chem. Soc.* **2002**, *124*, 11064−11072.
(13) Ishi-i, T.; Crego-Calama, M.; Timmerman, P.; Reinhoudt, D. N.; Shinkai, S. *Angew. Chem., Int. Ed.* **2002**, *41*, 1924−1929.
(14) Oda, R.; Huc, I.; Schmutz, M.; Candau, S. J.; MacKintosh, F. C. *Nature* **1999**, *399*, 566−569.
(15) El-Hachemi, Z.; Mancini, G.; Rib, J. M.; Sorrenti, A. *J. Am. Chem. Soc.* **2008**, *130*, 15176−15184.
(16) (a) Palmans, A. R. A.; Vekemans, J. A. J. M.; Havinga, E. E.; Meijer, E. W. *Angew. Chem., Int. Ed.* **1997**, *36*, 2648. (b) von Berlepsch, H.; Kirstein, S.; Buttcher, C. *J. Phys. Chem. B.* **2003**, *107*, 9646. (c) Ghosh, S.; Li, X.-Q.; Stepanenko, V.; Würthner, F. *Chem.—Eur. J.* **2008**, *14*, 11343. (d) Kawagoe, Y.; Fujiki, M.; Nakano, Y. *New. J. Chem.* **2010**, *34*, 637. (e) Isare, B.; Linares, M.; Zargarian, L.; Fermandjian, S.; Miura, M.; Motohashi, S.; Vanthuyne, N.; Lazzaroni, R.; Bouteiller, L. *Chem.—Eur. J.* **2010**, *16*, 173. (f) George, S. J.; Tomovic, Z.; Schenning, A. P. H. J.; Meijer, E. W. *Chem. Commun.* **2011**, *47*, 3451. (g) Zhang, W.; Fujiki, M.; Zhu, X.-L. *Chem.—Eur. J.* **2011**, *17*, 10628−10635. (h) Xiao, J.; Xu, J.; Cui, S.; Liu, H.; Wang, S.; Li, Y. *Org. Lett.* **2008**, *10*, 645−648. (i) Molla, M. R.; Das, A.; Ghosh, S. *Chem. Commun.* **2011**, *47*, 8934−8936. (j) Huang, Y.; Hu, J.; Kuang, W.; Wei, Z.; Faul, C. F. J. *Chem. Commun.* **2011**, *47*, 5554−5556. (k) Seki, T.; Asano, A.; Shu, S.; Kikkawa, Y.; Murayama, H.; Karatsu, T.; Kitamura, A.; Yagai, S. *Chem.—Eur. J.* **2011**, *17*, 3598−3608.
(17) (a) Prins, L. J.; De Jong, F.; Timmerman, P.; Reinhoudt, D. N. *Nature* **2000**, *408*, 181−184. (b) Ishi-i, T.; Crego-Calama, M.; Timmerman, P.; Reinhoudt, D. N.; Shinkai, S. *J. Am. Chem. Soc.* **2002**, *124*, 14631−14641. (c) Zhao, J.-S.; Ruan, Y.-B.; Jiang, Y.-B. *Chem. Sci.* **2011**, *2*, 937.
(18) Rosaria, L.; D'urso, A.; Mammana, A.; Purrello, R. *Chirality* **2008**, *20*, 411−419.
(19) Lauceri, R.; Raudino, A.; Scolaro, L. M.; Micali, N.; Purrello, R. *J. Am. Chem. Soc.* **2002**, *124*, 894−895.
(20) Mammana, A.; D'Urso, A.; Lauceri, R.; Purrello, R. *J. Am. Chem. Soc.* **2007**, *129*, 8062−8063.
(21) Helmich, F.; Lee, C. C.; Schenning, A. P. H. J.; Meijer, E. W. *J. Am. Chem. Soc.* **2010**, *132*, 16753−16755.
(22) Schenning, A. P. H. J.; Jonkheijm, P.; Peeters, E.; Meijer, E. W. *J. Am. Chem. Soc.* **2001**, *123*, 409−416.
(23) Jonkheijm, P.; van der Schoot, P.; Schenning, A. P. H. J.; Meijer, E. W. *Science* **2006**, *313*, 80−83.
(24) (a) De Cat, I.; Guo, Z.; George, S. J.; Meijer, E. W.; Schenning, A.P.H. J.; De Feyter, S. *J. Am. Chem. Soc.* **2012**, *134*, 3171−3177. (b) Korevaar, P. A.; George, S. J.; Markvoort, A. J.; Smulders, M. M. J.; Hilbers, P. A. J.; Schenning, A. P. H. J.; De Greef, T. F. A.; Meijer, E. W. *Nature* **2012**, *481*, 492−496.
(25) Hoeben, F. J. M.; Herz, L. M.; Daniel, C.; Jonkheijm, P.; Schenning, A. P. H. J.; Silva, C.; Meskers, S. C. J.; Beljonne, D.; Phillips, R. T.; Friend, R. H.; Meijer, E. W. *Angew. Chem., Int. Ed.* **2004**, *43*, 1976−1979.
(26) Elbe, F.; Keck, J.; Fluegge, A. P.; Kramer, H. E. A.; Fischer, P.; Hayoz, P.; Leppard, D.; Rytz, G.; Kaim, W.; Ketterle, M. *J. Phys. Chem. A* **2000**, *104*, 8296−8306.
(27) Kolthoff, I. M. *Anal. Chem.* **1974**, *46*, 1992−2003.
(28) pK_a of TA is 3.4 which leads to a stronger hydrogen-bonded ion pair interaction with OPVs, whereas citronellic acid (CA, see ref 11) molecules (pK_a = 5.2) interact through only weak hydrogen bonded interactions.
(29) Green, M. M.; Peterson, N. C.; Sato, T.; Teramoto, A.; Cook, R.; Lifson, S. *Science* **1995**, *268*, 1860−1866.
(30) Palmans, A. R. A.; Meijer, E. W. *Angew. Chem. Int. Ed* . **2007**, *46*, 8948−8968.
(31) Smulders, M. M. J.; Schenning, A. P. H. J.; Meijer, E. W. *J. Am. Chem. Soc.* **2008**, *130*, 606−611.
(32) Barbera, J.; Puig, L.; Romero, P.; Serrano, J. L.; Sierra, T. *J. Am. Chem. Soc.* **2005**, *127*, 458−464.
(33) Gawronski, J.; Gawroska, K.; Skowronek, P.; Rychlewska, U.; Warajtis, B.; Rychlewski, J.; Hoffmann, M.; Szarecka, A. *Tetrahedron* **1997**, *53*, 6113−6144.
(34) Although similar chiral memory could be introduced in so-called AOPV4 stacks (see ref 23) by a chiral supramolecular auxiliary, a detailed kinetic analysis was hampered by the precipitation of the compound inside the cuvette. However, analysis of the kinetic data based on the *g*-value showed enough kinetic stability at room temperature. See Figure S12 of the Supporting Information.
(35) Mayo, S. L.; Olafson, B. D.; Goddard, W. A., III *J. Phys. Chem.* **1990**, *94*, 8897−8909.